

Fourier Transform Infrared Observation of SiC_n Chains. II. The $\nu_1(\sigma)$ Mode of Linear SiC₇ in Ar at 10 K[†]

X. D. Ding, S. L. Wang,[‡] C. M. L. Rittby, and W. R. M. Graham^{*,§}

Department of Physics and Astronomy, Texas Christian University, Fort Worth, Texas 76129

Received: October 29, 1999

The linear SiC₇ cluster has been detected for the first time in Fourier transform infrared spectra observed when the products from the laser evaporation of Si/C rods were trapped in Ar at ~10 K. Comparison of ¹³C isotopic shift measurements with the results of density functional theory (DFT) calculations confirms the identification of the $\nu_1(\sigma)$ mode of SiC₇ at 2100.8 cm⁻¹.

Introduction

Silicon–carbon clusters are potentially important in astrophysics, especially carbon chains with a Si atom at one or both ends because many stellar and circumstellar molecules have a carbon chain backbone. In particular, the SiC_n clusters, SiC,¹ SiC₂,^{2,3} SiC₃,⁴ and SiC₄,⁵ have been observed by means of their rotational spectra in the circumstellar shell of the carbon star IRC +10216.

Previously we have reported vibrational spectra for the SiC₃–Si,⁶ SiC₄,⁷ and SiC₄Si⁸ silicon–carbon chains formed by trapping the products of Knudsen cell evaporation in solid Ar. Recently, using the laser ablation technique, we have extended our investigations to linear SiC_n clusters with $n > 4$, and have reported the detection of SiC₉.⁹ Excellent agreement between frequency and isotopic shifts measured with FTIR (Fourier transform infrared) spectroscopy and the predictions of B3LYP/cc-pVDZ (Becke II–Lee–Yang–Parr functional with correlation consistent polarized valence double- ζ basis set) DFT calculations resulted in the identification of the $\nu_4(\sigma)$ mode of SiC₉ at 1935.8 cm⁻¹ in Ar. The rotational spectra of four other SiC_n chain molecules, SiC₄, SiC₅, SiC₆, and SiC₈, formed by an electric discharge in a supersonic molecular beam of silane and diacetylene have been detected using Fourier transform microwave spectroscopy.¹⁰

As a part of our continuing FTIR matrix studies of the vibrational spectra of SiC_n clusters formed by laser ablation, we report the detection of another new species, linear SiC₇. Although no theoretical calculations had been reported prior to the present study, it was expected that SiC₇, like C₇, would be linear because experimental and theoretical evidence had suggested that the original linear carbon chain structure is retained on the addition of a Si atom to one or both ends of C₄ (ref 7, 11), C₅ (ref 12), and C₉ (ref 9) chains. Based on a comparison of measured ¹³C isotopic shifts with the results of DFT calculations, the $\nu_1(\sigma)$ mode of SiC₇ has been assigned.

Theoretical Calculations

To aid in the identification of the vibrational spectrum of linear SiC₇, we have performed a series of density functional

TABLE 1: B3LYP/cc-pVDZ Optimized Geometry Parameters for Linear SiC₇^a

bond	parameter value (Å)
Si–C1	1.735
C1–C2	1.287
C2–C3	1.294
C3–C4	1.285
C4–C5	1.284
C5–C6	1.300
C6–C7	1.300

^a The equilibrium rotational constant for this geometry is $B_e = 0.415$ GHz with a dipole moment of $\mu = 7.29$ D.

TABLE 2: B3LYP/cc-pVDZ Harmonic Frequencies and Infrared Intensities for Linear SiC₇

vibrational mode	harmonic frequency (cm ⁻¹)	infrared intensity (km/mol)
$\nu_1(\sigma)$	2134	1595
$\nu_2(\sigma)$	2094	11.5
$\nu_3(\sigma)$	1949	140
$\nu_4(\sigma)$	1632	310
$\nu_5(\sigma)$	1202	8.9
$\nu_6(\sigma)$	771	19.3
$\nu_7(\sigma)$	414	12.5
$\nu_8(\pi)$	676	0.2
$\nu_9(\pi)$	557	0.7
$\nu_{10}(\pi)$	396	4.3
$\nu_{11}(\pi)$	246	0.8
$\nu_{12}(\pi)$	137	6.8
$\nu_{13}(\pi)$	53	0.9

calculations at the standard B3LYP/cc-pVDZ level using the *Gaussian 94*/DFT program suite.¹³ Vibrational fundamentals, infrared intensities, and isotopic shifts were calculated for linear SiC_n and SiC_nSi ($5 \leq n \leq 9$) clusters for selected fundamentals in the frequency range of interest. These calculations gave us an overview of the expected isotopic shift patterns to compare with experiment. Through the process of identification presented below an observed absorption was identified as originating from linear SiC₇. The optimized geometry parameters along with the predicted dipole moment and rotational constant for the ³Σ ground state of linear SiC₇ are given in Table 1. For a comparison of rotational constants and dipole moments with other SiC_n clusters see our earlier paper on the detection of SiC₉.⁹ The harmonic fundamental frequencies and infrared intensities of linear SiC₇ are given in Table 2. Since the bending fundamentals are of very low absolute intensity and thus unlikely

[†] Part of the special issue “Marilyn Jacox Festschrift”.

[‡] Current address: Bruker Optics, 47697 Westinghouse Drive, Fremont, CA 94539

[§] Please address any e-mail correspondence to: w.graham@tcu.edu and m.rittby@tcu.edu

TABLE 3: B3LYP/cc-pVDZ Singly Substituted Isotopic Shift Frequencies (cm⁻¹) for the σ Modes of Linear SiC₇

isotopomer	ν_1	ν_2	ν_3	ν_4	ν_5	ν_6	ν_7
Si-C-C-C-C-C-C-C							
28-12-12-12-12-12-12-12	2134.3	2093.6	1949.1	1632.5	1201.5	771.0	413.7
28-13-12-12-12-12-12-12	2131.2	2093.0	1935.7	1616.5	1188.2	767.3	413.1
28-12-13-12-12-12-12-12	2127.6	2081.1	1922.0	1631.0	1197.2	765.0	413.6
28-12-12-13-12-12-12-12	2133.9	2057.6	1949.0	1615.9	1200.5	765.8	413.6
28-12-12-12-13-12-12-12	2127.5	2063.5	1940.8	1631.5	1190.2	769.2	413.1
28-12-12-12-12-13-12-12	2105.1	2087.8	1947.7	1619.1	1193.5	771.0	412.3
28-12-12-12-12-12-13-12	2118.4	2090.7	1923.9	1624.5	1201.5	768.6	411.3
28-12-12-12-12-12-12-13	2132.3	2092.6	1942.1	1622.0	1191.5	764.4	410.7
29-12-12-12-12-12-12-12	2134.3	2093.6	1949.0	1632.3	1200.8	768.5	410.0
30-12-12-12-12-12-12-12	2134.3	2093.6	1949.0	1632.2	1200.2	766.1	406.4

TABLE 4: Comparison of Observed Vibrational Frequencies (cm⁻¹) of the $\nu_1(\sigma)$ Mode for ¹³C Substituted Isotopomers of SiC₇ with the Predictions of B3LYP/cc-pVDZ Calculations

isotopomer		observed	B3LYP/cc-pVDZ	scaled ^a	difference
Si-C-C-C-C-C-C-C		ν	ν	ν	$\Delta\nu$
28-12-12-12-12-12-12-12	(A)	2100.8	2134.3	2100.8	0.0
28-13-12-12-12-12-12-12	(B)	2098.4	2131.2	2097.7	0.7
28-12-13-12-12-12-12-12	(C)	2093.8	2127.6	2094.2	-0.4
28-12-12-13-12-12-12-12	(D)	overlapped ^b	2133.9	2100.4	
28-12-12-12-13-12-12-12	(E)	2093.2	2127.5	2094.1	-0.9
28-12-12-12-12-13-12-12	(F)	2072.3	2105.1	2072.1	0.2
28-12-12-12-12-12-13-12	(G)	overlapped ^c	2118.4	2085.1	
28-12-12-12-12-12-12-13	(H)	2099.8	2132.3	2098.8	1.0

^a Results of the B3LYP/cc-pVDZ calculation scaled by a factor of 2100.8/2134.3. ^b Possibly overlapped by the main band at 2100.8 cm⁻¹. ^c Possibly overlapped by a band at 2086.8 cm⁻¹, see text for detail.

TABLE 5: B3LYP/cc-pVDZ Predicted Singly Substituted ¹³C Shifts for IR Active Modes of SiC_nSi and SiC_n Chains (5 ≤ n ≤ 9) at Frequencies of $\omega \geq 2000$ cm⁻¹

species	mode	freq (cm ⁻¹)	IR intensity (km mol ⁻¹)	scaled ^a isotopic shifts (cm ⁻¹)									
SiC ₅ Si	$\nu_4(\sigma_u)$	2155.2	4838	1.4	15.5	37.9							
SiC ₆ Si	$\nu_5(\sigma_u)$	2079.3	516	1.4	7.2	9.1							
SiC ₇ Si	$\nu_5(\sigma_u)$	2154.4	5506	0.4	2.9	27.6	37.3						
SiC ₈ Si	$\nu_6(\sigma_u)$	2149.9	1073	1.1	3.0	9.5	18.2						
SiC ₉ Si	$\nu_6(\sigma_u)$	2177.3	600	0.0	2.8	6.4	16.4	32.2					
	$\nu_7(\sigma_u)$	2031.2	15702	0.9	1.0	5.4	10.8	21.0					
SiC ₅	$\nu_1(\sigma)$	2116.3	315	1.5	2.8	14.2	19.7	35.1					
SiC ₆	$\nu_1(\sigma)$	2225.1	4694	0.1	1.4	3.7	9.6	23.9	30.6				
	$\nu_2(\sigma)$	2140.8	108	4.9	5.9	9.7	13.1	23.0	30.5				
SiC ₇	$\nu_1(\sigma)$	2134.3	1595	0.4	2.0	3.1	6.6	6.7	15.7	28.7			
	$\nu_2(\sigma)$	2093.6	11.5	0.7	1.0	2.9	5.8	12.5	30.2	36.1			
SiC ₈	$\nu_1(\sigma)$	2240.9	958	0.0	1.9	2.2	5.5	8.2	9.7	12.3	24.8		
	$\nu_2(\sigma)$	2191.6	4141	0.2	0.8	1.5	1.6	3.3	21.8	23.0	34.5		
	$\nu_3(\sigma)$	2057.4	5854	1.6	1.9	5.8	6.2	8.3	8.8	23.1	27.3		
SiC ₉	$\nu_1(\sigma)$	2176.4	2278	0.2	0.3	0.8	3.7	5.8	6.6	12.4	13.5	21.4	
	$\nu_2(\sigma)$	2129.3	4.8	0.5	2.1	2.5	4.2	9.1	10.4	10.5	12.9	27.8	
	$\nu_3(\sigma)$	2005.4	495	0.3	1.6	3.6	4.6	7.1	9.8	12.6	16.7	25.3	
	observed shifts			1.0	2.4	7.0	7.6	ol ^b	28.5				

^a The scale factor is the 2100.8 cm⁻¹ frequency of the observed absorption divided by the predicted frequency of the mode. ^b Possibly overlapped by a band at 2086.8 cm⁻¹, see text for detail.

to be observed in our experiment, we present isotopic shifts for only the stretching fundamentals in Table 3. The additional results presented in Tables 4–6 are discussed in the analysis of the experimental spectrum below.

Experimental Procedure

Figure 1 schematically shows our two-laser ablation system setup. Two sample rods are simultaneously vaporized using two focused Nd:YAG (GCR-11, Spectra-Physics) pulsed lasers operating at 1064 nm so that the experimental parameters, such as laser power, laser focus, can be adjusted separately to accommodate the different evaporation characteristics of the two materials. Various rods were used for the present work including commercially purchased graphite (National Carbon Company,

TABLE 6: B3LYP/cc-pVDZ Harmonic Frequencies and Infrared Intensities for Linear SiC₆

vibrational mode	harmonic frequency	infrared intensity
	(cm ⁻¹)	(km/mol)
$\nu_1(\sigma)$	2225.1	4694
$\nu_2(\sigma)$	2140.8	108
$\nu_3(\sigma)$	1877.3	1275
$\nu_4(\sigma)$	1380.2	55
$\nu_5(\sigma)$	889.0	54
$\nu_6(\sigma)$	461.2	25
$\nu_7(\pi)$	683.8	6.8
$\nu_8(\pi)$	548.4	3.2
$\nu_9(\pi)$	277.9	0.5
$\nu_{10}(\pi)$	159.5	9.0
$\nu_{11}(\pi)$	63.0	0.5

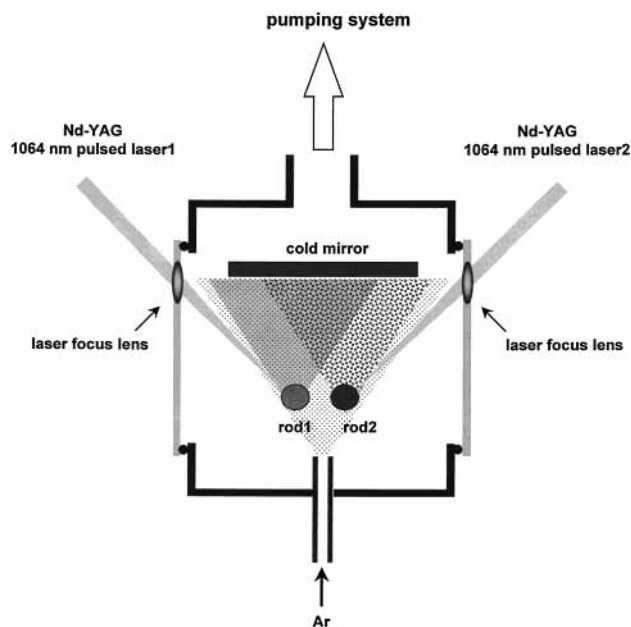


Figure 1. Configuration of the dual-laser ablation system.

99.999% purity), Si (ESPI, 99.9999% purity), and SiC rods (CERAC, 99.5% purity), as well as rods fabricated in this laboratory by compressing a mixture of silicon (Alfa, 99.999% purity) and graphite (Alfa, 99.9995% purity) powder under high pressure. The latter could be made with any desired Si/C ratio or ^{13}C enrichment (Isotec, 99.3% purity). A degassing procedure was used to remove any trapped gas by heating the rods to $\sim 200^\circ\text{C}$ under vacuum for more than 24 h.

The evaporated species were condensed in solid Ar (Matheson, 99.9995% purity) on a gold plated surface which was

cooled to $\sim 10\text{ K}$ by a closed cycle refrigerator (APD Cryogenics, Displex) in a vacuum maintained at 10^{-7} Torr or better. If necessary, spectra were improved by annealing in order to sharpen absorption lines or to enhance the yield of a particular species by diffusion in the matrix. During annealing the cold mirror was warmed to a temperature between 20 and 50 K where it was maintained for ~ 10 min before cooling back to $\sim 10\text{ K}$.

FTIR absorption spectra of the matrix samples were recorded in the region of $550\text{--}3900\text{ cm}^{-1}$ at a resolution of 0.2 cm^{-1} using a Bomem DA 3.16 Fourier transform spectrometer equipped with a liquid nitrogen cooled MCT (Hg–Cd–Te) detector and KBr beam splitter. Details of the optical system have been reported previously.¹⁴ All frequencies reported were measured to $\pm 0.1\text{ cm}^{-1}$.

Results and Discussion

Figure 2 shows three FTIR spectra obtained using the two-laser ablation system in the region near 2000 cm^{-1} , where most of the stretching modes of silicon–carbon clusters are expected to be located. The middle and bottom spectra were observed when C (containing 1% ^{13}C in natural abundance) and Si rods were evaporated simultaneously. The bottom spectrum was typically observed at somewhat higher laser power levels than for the middle spectrum, and is characterized by more intense bands of C_3 , C_6 , C_7 , and C_9 . The top spectrum in Figure 2, produced by the evaporation of a single C rod, is provided for comparison.

As expected, almost all of the C_n clusters observed in the pure carbon cluster spectrum at the top of Figure 2 also appear in the silicon–carbon cluster spectra (middle and bottom of Figure 2) since all three involve the evaporation of a carbon rod. The simultaneous evaporation of a SiC rod for the middle and bottom spectra, however, produced characteristic vibrations

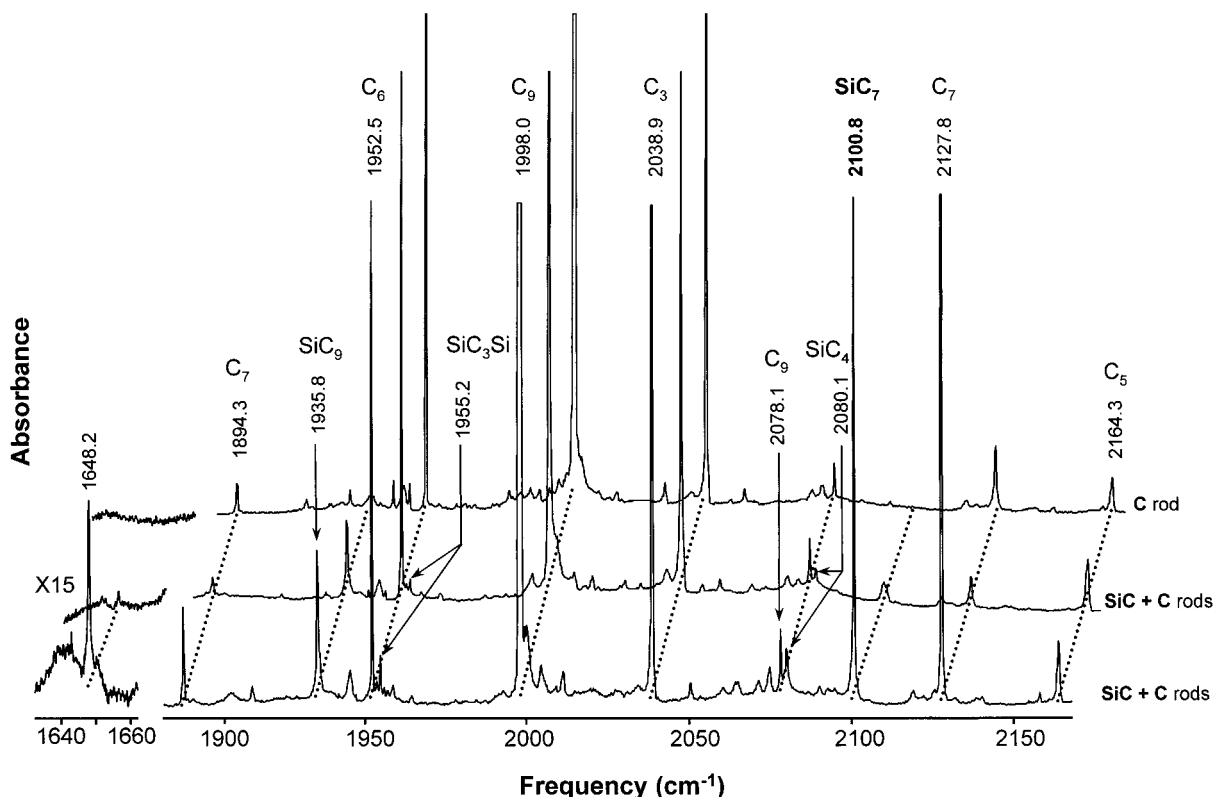


Figure 2. Typical FTIR spectra of pure carbon clusters produced by the laser evaporation of a single C rod (top), and silicon–carbon clusters produced by the laser evaporation of a pair of C and SiC rods evaporated at low (middle) and high power (bottom). The middle and top spectra are shifted slightly to higher frequency to avoid overlapping absorptions.

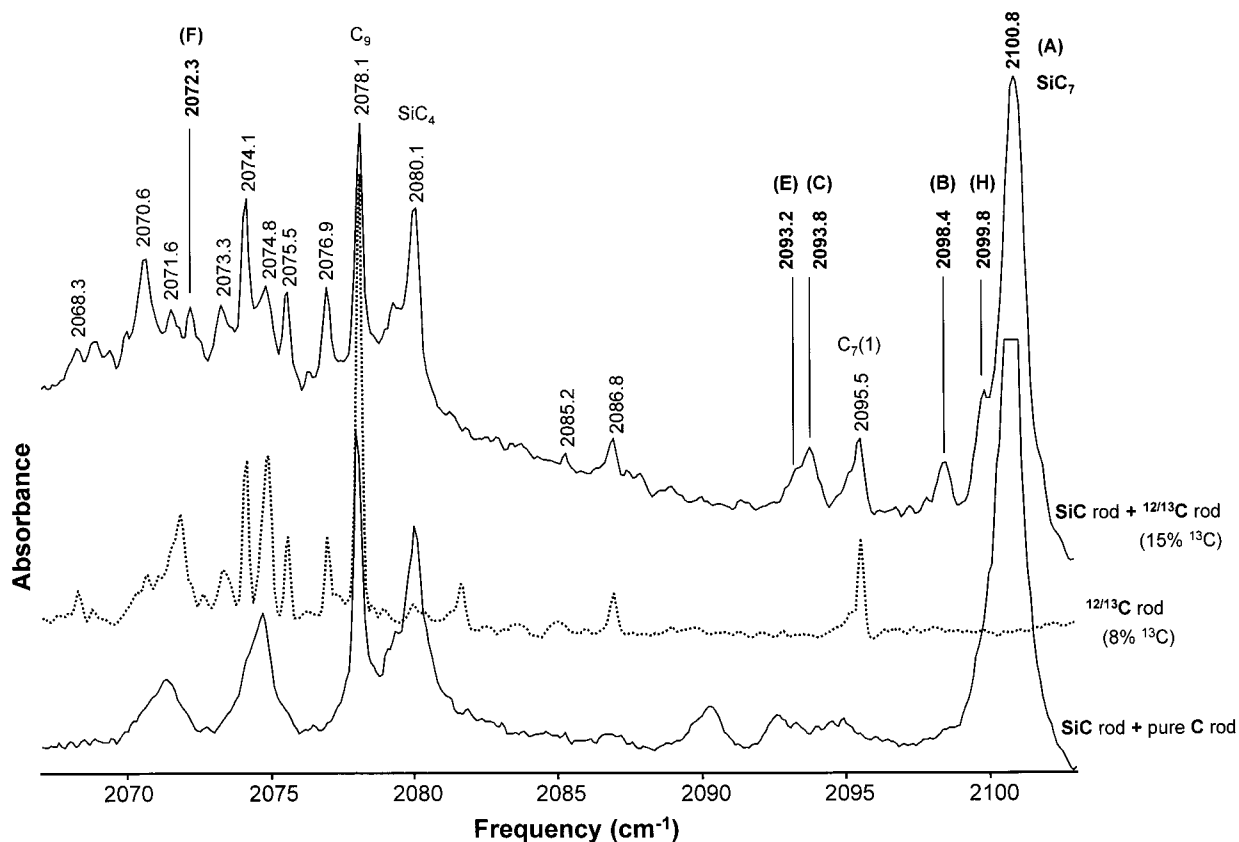


Figure 3. Comparison of FTIR spectra produced by the evaporation of three different sets of sample rods: a SiC rod and a C rod with 1% ¹³C in natural abundance (bottom), a C rod with 8% ¹³C isotopic enrichment (middle), and a SiC (1% ¹³C) rod and a C rod with 15% ¹³C isotopic enrichment (top). The letters identifying the isotopomer bands of SiC₇ correspond to the labeling scheme shown in Table 4.

of silicon–carbon clusters, the $\nu_3(\sigma_u) = 1955.2 \text{ cm}^{-1}$ mode of SiC₃Si,⁶ the $\nu_1(\sigma) = 2080.1 \text{ cm}^{-1}$ mode of SiC₄,⁷ and the $\nu_4(\sigma) = 1935.8 \text{ cm}^{-1}$ mode of SiC₉,⁹ which have all been reported previously by this lab.

In addition, a new, extremely intense absorption at 2100.8 cm^{-1} was observed in the silicon–carbon cluster spectrum (bottom, Figure 2). Since this band, like the other silicon–carbon cluster bands, appears only when Si is present, the molecule responsible must contain silicon. The possibility that it is a band of a contaminant species can be easily eliminated because other benchmark contaminants such as SiH₄, SiCO, SiN₂, CO, and CO₂ are very weak. Another possibility is that the carrier of the 2100.8 cm^{-1} absorption is a pure silicon cluster; however, this is unlikely since the vibrational modes for the pure silicon clusters^{15,16} (Si_n, $n = 2-8$) have been predicted and, in many cases, observed¹⁷ to lie below 700 cm^{-1} . Thus, a silicon–carbon cluster is the most plausible candidate for the carrier of the 2100.8 cm^{-1} absorption.

From our experiments, it was found that the intensity of the 2100.8 cm^{-1} band is correlated with the intensity of the $\nu_4(\sigma_u)$ mode of C₇ at 2127.8 cm^{-1} . This is illustrated by Figure 2 where both bands are intense in the bottom spectrum, and both weak in the middle spectrum. This intensity correlation suggests the possibility that the silicon–carbon cluster responsible for the 2100.8 cm^{-1} absorption may derive from the C₇ chain and be of the form SiC₇ or SiC₇Si.

Figure 3 shows three FTIR spectra in the region near 2100.8 cm^{-1} . The bottom spectrum, which is an expanded portion of the bottom spectrum shown in Figure 2, was produced from the simultaneous laser ablation of a pure C rod and a SiC rod, and is dominated by strong bands of the unknown silicon–carbon cluster at 2100.8 cm^{-1} and the $\nu_5(\sigma_u)$ band of linear C₉

at 2078.1 cm^{-1} . Since in both rods there is only the 1% natural abundance of the ¹³C isotope, no ¹³C-substituted isotopomers of any pure carbon cluster or silicon–carbon cluster appear in this spectrum. The middle spectrum was recorded using a single carbon rod, which was fabricated under pressure from graphite powder with 8% ¹³C. This level of ¹³C enrichment results in the appearance of absorptions from ¹³C-substituted isotopomers of pure carbon clusters, particularly to the low-frequency side of the ν_5 mode of C₉. In the absence of Si, however, no silicon–carbon clusters are observed, and, most importantly, the 2100.8 cm^{-1} band is absent. The top spectrum in Figure 3 was produced by the simultaneous ablation of a SiC rod and a carbon rod fabricated from graphite powder with 15% ¹³C enrichment. The presence of Si and 15% ¹³C isotopic enrichment in the ablation targets again results in the presence of ¹³C isotopomer absorptions of pure carbon clusters in the spectrum shown. The known single ¹³C substituted shifts at 2070.7 and 2075.0 cm^{-1} of the relatively weak SiC₄ absorption at 2080.0 cm^{-1} are overlapped by ¹³C isotopomer bands of the ν_5 mode of C₉. However, in other regions of the top spectrum, which are not shown in Figure 3, single ¹³C-substituted isotopomer bands of the SiC₃Si⁶ and SiC₉⁹ clusters are clearly observed. More importantly, new bands arising from the ¹³C enrichment also appear to the low-frequency side of the 2100.8 cm^{-1} band of the unknown silicon–carbon species. By comparing the top spectrum showing ¹³C isotopic shifts for both silicon–carbon and carbon clusters with the middle spectrum exhibiting shifts for only pure carbon clusters, it is then possible to identify potential ¹³C isotopic shifts for the 2100.8 cm^{-1} band. It is readily apparent that the 2099.9, 2098.4, 2093.8, 2093.2, and 2072.3 cm^{-1} bands in the top spectrum in Figure 3 are the ¹³C isotopic shifts for one or more silicon–carbon clusters. Since the 2100.8 cm^{-1} band is the only

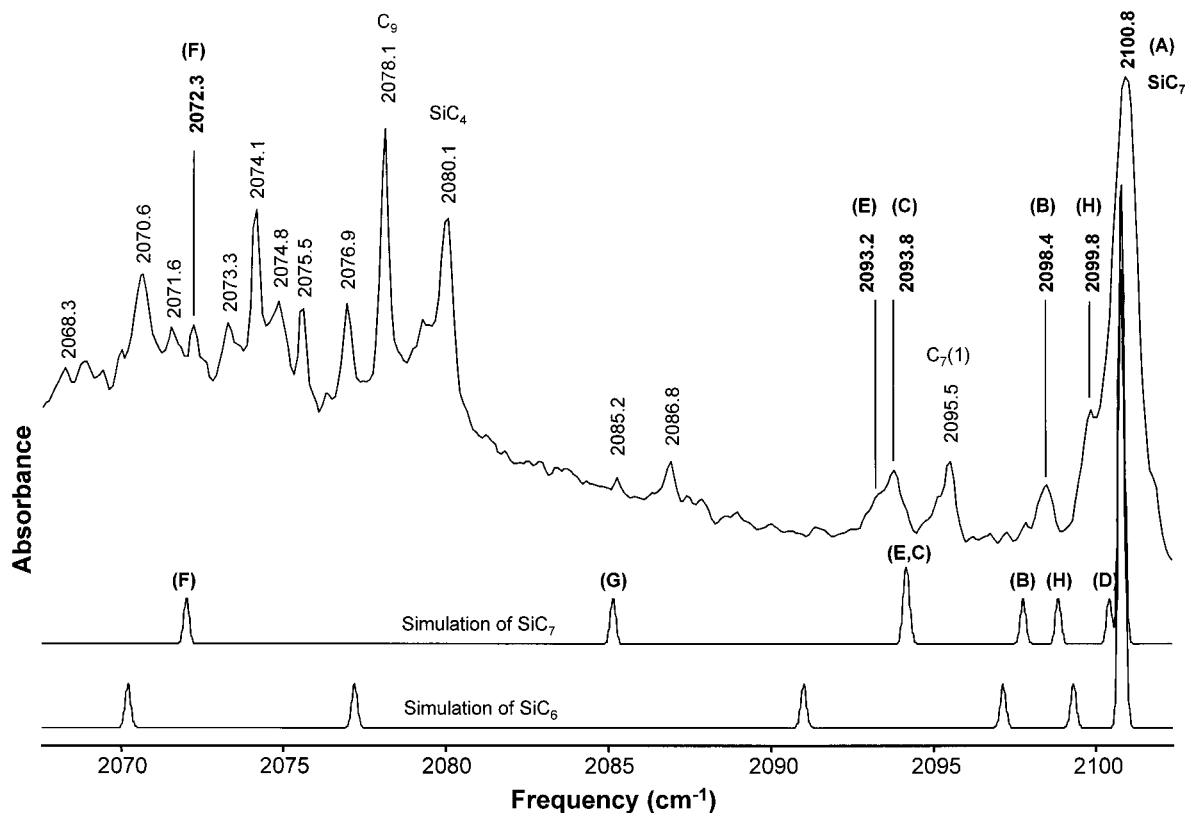


Figure 4. Comparison of observed isotopic shift spectrum (top) with simulated isotopic shift spectra (with 15% ^{13}C enrichment) for the ν_1 mode of SiC_7 (middle) and the ν_1 mode of SiC_6 (bottom). The letters identifying the isotopomer bands of SiC_7 correspond to the labeling scheme shown in Table 4.

nearby silicon–carbon absorption, all five absorptions are candidates for its isotopic shifts. Moreover, the relatively low ^{13}C isotopic enrichment restricts the spectrum to shifts for single ^{13}C substitutions only.

Based on the correlation of the intensities of the $\nu_4(\sigma_u)$ mode of C_7 at 2127.8 cm^{-1} and the unidentified 2100.8 cm^{-1} band, we have argued that the leading candidates for the carrier are SiC_7Si and SiC_7 . The existence of five ^{13}C isotopic shifts excludes SiC_7Si as a possible candidate, leaving SiC_7 as the likeliest carrier of the 2100.8 cm^{-1} band. As can be seen from Table 2, which shows the frequencies of the σ modes of SiC_7 and their isotopic shifts calculated at the B3LYP/cc-pVDZ level, $\nu_1(\sigma)$ is predicted to be the most intense. Its frequency of 2134 cm^{-1} is very close to the 2100.8 cm^{-1} absorption. Furthermore, careful examination of the ^{13}C isotopic shift patterns in Table 3 predicted for all of the SiC_7 stretching modes shows that the pattern for the ν_1 mode of SiC_7 is uniquely close to the shifts observed for the 2100.8 cm^{-1} band.

A comparison between the observed isotopomer frequencies and the B3LYP/cc-pVDZ predictions is shown in Table 4. Five of the frequencies are in excellent agreement with the predicted values for the isotopomers labeled B, C, E, F, and H. The D isotopomer with a predicted shift of 0.4 cm^{-1} would be overlapped by the envelope of the main band. Although a band at 2085.2 cm^{-1} is very close to the predicted 2085.1 cm^{-1} frequency of isotopomer G, it is an unlikely candidate since its intensity is anomalously weak compared to the other isotopomer bands, and in some experiments it is not detectable. It is much more likely that a pure carbon band at 2086.8 cm^{-1} , about 1.7 cm^{-1} higher than the predicted frequency of 2085.1 cm^{-1} , overlaps the isotopomer G band. It should be noted that the ^{29}Si and ^{30}Si isotopic shifts for the ν_1 mode arising from their respective 4.7% and 3.1% natural abundances are not observable

because, as shown in Table 3, their predicted shifts of less than 0.1 cm^{-1} would be overlapped by the main band.

Although the agreement between the observed and calculated isotopic shifts for the assignment of the 2100.8 cm^{-1} frequency to the ν_1 mode of SiC_7 is very good, we have carefully examined possible alternative assignments to other SiC_n and SiC_nSi chains. Table 5 shows the frequencies of the σ modes and their isotopic shifts calculated for all linear SiC_n and SiC_nSi ($5 \leq n \leq 9$) clusters at the B3LYP/cc-pVDZ level. Comparison of all these predicted isotopic shifts with the observed isotopomer bands indicates that, except for the ν_1 mode of SiC_7 and the ν_1 mode of SiC_6 predicted at 2225.1 cm^{-1} , none of the others even approximately fit the experimental data. Although there appears to be no correlation between the 2100.8 cm^{-1} band and the intensity of the $\nu_5(\sigma_u)$ band of C_6 at 1952.5 cm^{-1} in Figure 2, C_6 is certainly an abundant product of the laser ablation of C rods. To further test the ν_1 mode of SiC_6 as an alternative assignment, we have plotted the simulated isotopic spectra for both modes together with the observed isotopic spectrum in Figure 4. These spectra graphically demonstrate that the predicted isotopic shifts for the ν_1 mode of SiC_7 match the observed shifts much better than those for the ν_1 mode of SiC_6 .

Further evidence for the assignment to SiC_7 , is the observation of a silicon–carbon cluster band at 1648.2 cm^{-1} which, as shown in Figure 2, is correlated in intensity with the 2100.8 cm^{-1} band during annealing. As can be seen from Table 2, the frequency of the 1648.2 cm^{-1} absorption is very close to the 1632 cm^{-1} calculated for $\nu_4(\sigma)$, predicted to be the second most intense mode of SiC_7 . Unfortunately, the 1648.2 cm^{-1} absorption is too weak to observe ^{13}C isotopic shifts, which would confirm this tentative assignment. However, it is important to note that in contrast to SiC_7 , SiC_6 is predicted to have no mode with a frequency close to the 1648.2 cm^{-1} absorption. Moreover, there

is no evidence in our spectra of a silicon–carbon absorption near the 1877 cm⁻¹ frequency which is calculated for the second most intense mode of SiC₆, $\nu_3(\sigma)$ (as shown in Table 6).

The very good agreement between the B3LYP theoretical predictions and the observed mode frequency and ¹³C isotopic shifts (as shown in Table 4) strongly support the assignment of the 2100.8 cm⁻¹ absorption to the ν_1 mode of SiC₇.

Conclusion

The linear SiC₇ cluster produced by trapping the products of the laser evaporation of Si/C rods in an Ar matrix has been detected for the first time. FTIR measurements of the $\nu_1(\sigma)$ fundamental at 2100.8 cm⁻¹ and its ¹³C isotopic shifts are in excellent agreement with the predictions of B3LYP/cc-pVDZ DFT calculations. A second absorption at 1648.2 cm⁻¹ which is correlated in intensity to the $\nu_1(\sigma)$ may be the $\nu_4(\sigma)$ mode of SiC₇ which is predicted to be at 1632 cm⁻¹. In the absence of isotopic shifts, however, the assignment of the second mode must be considered very tentative.

Acknowledgment. Grants from the Welch Foundation (Graham, No. P-0786; Rittby, No. P-1259) and the TCU Research and Creative Activities Fund in support of this research, and from the W.M. Keck Foundation for the Bomem spectrometer, are gratefully acknowledged.

References and Notes

(1) Cernicharo, J.; Gottlieb, C. A.; Guelin, M.; Thaddeus, P.; Vrtilik, J. M. *Astrophys. J.* **1989**, *341*, L25.

- (2) Kleman, B. *Astrophys. J.* **1989**, *123*, 162.
(3) Thaddeus, P.; Cummins, S. E.; Linke, R. A. *Astrophys. J.* **1984**, *283*, L45.
(4) Apponi, A. J.; McCarthy, M. C.; Gottlieb, C. A.; Thaddeus, P. 54th Ohio State University International Symposium on Molecular Spectroscopy, Columbus, Ohio, June 1999; Paper No. TJ02.
(5) Ohishi, M.; Kaifu, N.; Kawaguchi, K.; Murakami, A.; Saito, S.; Yamamoto, S.; Ishikawa, S.; Fujita, Y.; Shiratori, Y.; Irvine, W. M. *Astrophys. J.* **1989**, *345*, L83.
(6) (a) Presilla-Márquez, J. D.; Graham, W. R. M. *J. Chem. Phys.* **1994**, *100*, 181. (b) Rittby, C. M. L. *J. Chem. Phys.* **1994**, *100*, 175.
(7) Withey, P. A.; Graham, W. R. M. *J. Chem. Phys.* **1992**, *96*, 4068.
(8) Presilla-Márquez, J. D.; Rittby, C. M. L.; Graham, W. R. M. *J. Chem. Phys.* **1997**, *106*, 8367.
(9) Ding, X. D.; Wang, S. L.; Rittby, C. M. L.; Graham, W. R. M. *J. Chem. Phys.* **1999**, *110*, 11214.
(10) Gordon, V.; Nathan, E.; Apponi, A. J.; McCarthy, M. C.; Gottlieb, C. A.; Thaddeus, P. 54th Ohio State University International Symposium on Molecular Spectroscopy, Columbus, Ohio, June 1999; Paper No. TJ01.
(11) Van Orden, A.; Provencal, R. A.; Giesen, T. F.; Saykally, R. J. *Chem. Phys. Lett.* **1995**, *237*, 77.
(12) Hunsicker, S.; Jones, R. O. *J. Chem. Phys.* **1996**, *105*, 5048.
(13) *Gaussian 94*, Revision E1; Frisch, M. J.; Trucks, G. W.; Schlegel, H. B.; Gill, P. M. W.; Johnson, B. G.; Robb, M. A.; Cheeseman, J. R.; Keith, T.; Petersson, G. A.; Montgomery, J. A.; Raghavachari, K.; Al-Laham, M. A.; Zakrzewski, V. G.; Ortiz, J. V.; Foresman, J. B.; Cioslowski, J.; Stefanov, B. B.; Nanayakkara, A.; Challacombe, M.; Peng, C. Y.; Ayala, P. Y.; Chen, W.; Wong, M. W.; Andres, J. L.; Replogle, E. S.; Gomperts, R.; Martin, R. L.; Fox, D. J.; Binkley, J. S.; Defrees, D. J.; Baker, J.; Stewart, J. P.; Head-Gordon, M.; Gonzalez, C.; Pople, J. A. Gaussian Inc.: Pittsburgh, PA, 1995.
(14) Shen, L. N.; Doyle, T. J.; Graham, W. R. M. *J. Phys. Chem.* **1990**, *93*, 1597.
(15) Raghavachari, K.; Rohlfing, C. M. *J. Chem. Phys.* **1988**, *89*, 2219.
(16) Fournier, R.; Sinnott, S. B.; DePristo, A. E. *J. Chem. Phys.* **1992**, *97*, 4149.
(17) Li, S.; Van Zee, R. J.; Weltner, W., Jr.; Raghavachari, K. *Chem. Phys. Lett.* **1995**, *243*, 275.